Chemistry & Biology
Article

LMP2-Specific Inhibitors: Chemical Genetic Tools for Proteasome Biology

Yik Khuan (Abby) Ho,[1] Paola Bargagna-Mohan,[2] Marie Wehenkel,[1] Royce Mohan,[1,2] and Kyung-Bo Kim[1,*]
[1] Department of Pharmaceutical Sciences
[2] Department of Ophthalmology and Visual Sciences
University of Kentucky, Lexington, KY 40536, USA
*Correspondence: kbkim2@uky.edu
DOI 10.1016/j.chembiol.2007.03.008

SUMMARY

The immunoproteasome, having been linked to neurodegenerative diseases and hematological cancers, has been shown to play an important role in MHC class I antigen presentation. However, its other pathophysiological functions are still not very well understood. This can be attributed mainly to a lack of appropriate molecular probes that can selectively modulate the immunoproteasome catalytic subunits. Herein, we report the development of molecular probes that selectively inhibit the major catalytic subunit, LMP2, of the immunoproteasome. We show that these compounds irreversibly modify the LMP2 subunit with high specificity. Importantly, LMP2-rich cancer cells compared to LMP2-deficient cancer cells are more sensitive to growth inhibition by the LMP2-specific inhibitor, implicating an important role of LMP2 in regulating cell growth of malignant tumors that highly express LMP2.

INTRODUCTION

In the era of proteomics, temporal and spatial control of protein functions, which are often difficult with conventional genetic manipulations, are critical to the understanding of the dynamics of cellular processes. While traditional genetic approaches have provided useful insight into the functions of proteins, they are limited by the possibility that some phenotypes may be due to compensatory responses that occur during development. In addition, the inhibition of the target gene function is often irreparable, and thus the desired protein deficiency cannot be readily regulated, making it difficult to dissect the precise roles of gene products. One way to complement classical genetic approaches is to use small molecules that selectively modulate protein functions. This small-molecule approach has increasingly contributed to further our understanding of biological processes.

The proteasome has emerged as a major player in many important signaling processes, such as cell cycle progression [1], inflammatory responses [2], and development [3]. Typically, more than 80% of cellular proteins are degraded by the ubiquitin-proteasome system. The ubiquitin-proteasome pathway is a highly regulated process in which proteins are first targeted for degradation by conjugation to ubiquitin, a 76 amino acid polypeptide. Ubiquitinated proteins are, in turn, recognized by the 19S regulatory domain of the constitutive 26S proteasome. Through a series of ATP hydrolysis-dependent processes, deubiquitinated proteins are threaded into the core proteolytic complex, the 20S proteasome, where they are degraded into small peptides. The 20S core has a four-ring stacked structure with seven different subunits in each ring. The two inner rings each contain three catalytically active β subunits. The noncatalytic outer α rings form a gated channel for unfolded protein entry and a base for the 19S regulatory complexes, which provide the specificity of the polypeptide recognition.

The 20S catalytic core proteasome has been shown to exhibit three major activities: a chymotrypsin-like (CT-L) activity that cleaves after large hydrophobic residues, a trypsin-like (T-L) activity that hydrolyzes after basic amino acids, and a caspase-like (C-L) activity that cleaves after acidic amino acids. Two other less-characterized catalytic activities have also been ascribed to the proteasome: BrAAP, which cleaves after branched-chain amino acids, and SNAAP, which cleaves after small, neutral amino acids. Although most efforts are directed to develop proteasome inhibitors against CT-L activity, a few studies have also been successful in designing compounds that inhibit other proteasomal activities, such as C-L [4] and T-L activity-specific inhibitors [5–8]. While the CT-L activity of the proteasome has been suggested to be largely responsible for the proteolytic function of the proteasome in vivo and in vitro [9, 10], the contribution of the other major activities remains to be determined. In recent years, researchers have been investigating the functions of the different proteolytic activities in cancer cells by using a variety of proteasome inhibitors [10, 11]. Regarding clinical applications of proteasome inhibitors, bortezomib (VELCADE), a broad-spectrum proteasome inhibitor targeting both the constitutive proteasome and immunoproteasomes, was recently approved by the FDA for the treatment of multiple myeloma (MM) [12]. However, its clinical use is severely limited due to drug-related toxicities [13].

In higher vertebrates, exposure of cells to stimuli, such as interferon (IFN)-γ or tumor necrosis factor (TNF)-α,

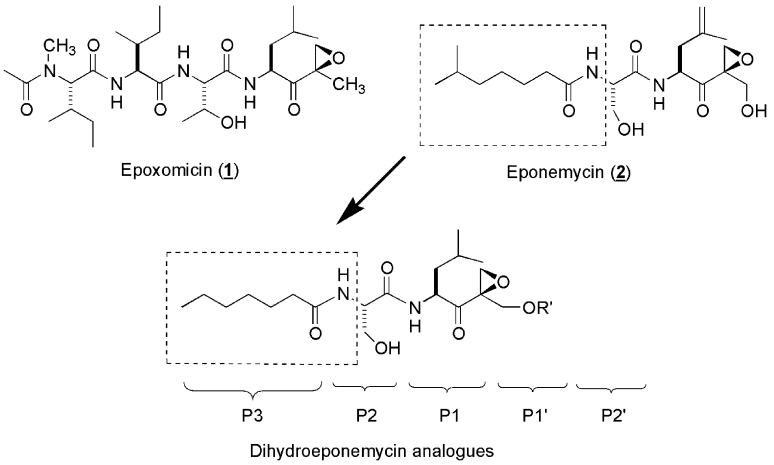

Figure 1. Structures of the α′,β′-Epoxyketone Linear Peptide Natural Product Epoxomicin and Dihydroeponemycin
Tripeptide epoxyketones with a linear hydrocarbon chain at the P3 position have higher specificity toward immunoproteasome catalytic subunits than normal tetrapeptide epoxyketones such as epoxomicin.

induces the synthesis of certain catalytic subunits (LMP7, LMP2, and MECL-1), which replace the constitutive β subunits X, Y, and Z, respectively, and form an alternative proteasome form known as the immunoproteasome [14]. The immunoproteasome, as compared to the constitutive (or regular) proteasome, has an enhanced capacity to generate peptides bearing hydrophobic and basic amino acids at their C termini and a reduced capacity to produce peptides bearing acidic residues at their C termini [15]. Consequently, the spectrum of the resultant peptides is shifted toward peptides that associate with MHC class I molecules with increased affinity [16]. While the immunoproteasome is suggested to play a major role in MHC class I antigen presentation, it is believed not to be solely responsible for antigen presentation, as the constitutive proteasome also generates immunogenic epitopes [17].

In recent years, questions regarding the role of the immunoproteasome in cells from nonimmune systems have arisen due to the findings in which expression levels of individual immunoproteasome subunits are correlated with pathological processes, such as hematological cancers and neurodegenerative diseases [18–20]. For instance, a high level of immunoproteasome catalytic subunits has been detected in neurodegenerative human brains [21, 22], which is known to be an immunologically privileged organ [23]. Specifically, the LMP2 catalytic subunit is more highly expressed in the brains of Alzheimer's disease (AD) patients than in the brains of nondemented elderly, whereas its expression in young brains is negligible or absent [24]. More recently, it has been shown that LMP2 is required for estrogen receptor-mediated gene transcription and for estrogen-stimulated cell cycle progression [25]. Further, some studies indicated that the immunoproteasome and its catalytic subunits may be involved in Huntington's disease (HD) neurodegeneration [21]. MM is also known to express a high level of immunoproteasome subunits due to the bone marrow microenvironment where it replicates [26–29]. Based on these observations, an intriguing hypothesis has been proposed that the specific inhibition of the immunoproteasome subunits may induce selective apoptosis of MM cells while sparing other cells lacking or minimally expressing immunoproteasome subunits [30], making them an attractive investigative target for clinical applications.

Despite the potential role of the immunoproteasome catalytic subunits in pathogenesis, their functions are still not fully understood. In addition, the catalytic activities of individual immunoproteasome subunits are not clearly characterized. The major problem that limits further understanding of immunoproteasome biology is the lack of appropriate molecular probes that selectively target the immunoproteasome catalytic subunits. Unfortunately, the proteasome inhibitors developed to date either preferentially target the constitutive proteasome subunits or fail to exhibit appropriate specificity toward the immunoproteasome subunits.

With this in mind, our ongoing efforts are aimed at the design and synthesis of small-molecule probes that selectively target the immunoproteasome catalytic subunits. While the sequence comparison of catalytic subunits from the constitutive proteasome and immunoproteasomes exhibits a high level of homology, structural information about the active sites of the immunoproteasome subunits remains to be elucidated, complicating our efforts toward the design of immunoproteasome subunit-specific probes via a rational target-based design strategy.

Two natural product proteasome inhibitors, epoxomicin and eponemycin (Figure 1), are members of the α′,β′-epoxyketone linear peptide family [31, 32]. It has been previously shown that, despite structural similarities, epoxomicin (**1**) and dihydroeponemycin (**2**), an active derivative of eponemycin, differ considerably in their proteasome subunit binding specificity [31, 32]. For example, dihydroeponemycin labels the catalytic threonine residues of the immunoproteasome subunits LMP2 and LMP7 and the constitutive proteasome subunit X. On the other hand, epoxomicin covalently modifies the N-terminal catalytic threonine residues of the constitutive proteasome (X and Z) and immunoproteasome (LMP7 and MECL1) subunits. We have previously shown that a relatively higher specificity of dihydroeponemycin

toward the immunoproteasome subunits (LMP2 and LMP7), as compared to epoxomicin, is due to a linear hydrocarbon residue at the N terminus (i.e., isooctanoic group) [33]. In addition, it has been suggested that amino acid residues at the P1′-P2′ sites (see Figure 1) of immunoproteasome substrates may also play an important role in immunoproteasome specificity [34]. We have also previously reported that serine at the P2 site of dihydroeponemycin can be replaced with alanine while maintaining the subunit-binding pattern of dihydroeponemycin [35].

Based on these observations, we would like to develop a new molecular probe that will selectively inactivate the catalytic threonine residue of immunoproteasome subunit LMP2 by derivatizing the P1′-OH group of dihydroeponemycin (Figure 1). We envision that LMP2 inhibitors that covalently modify the catalytic threonine residue of LMP2 will provide a valuable chemical genetic tool in the functional exploration of individual immunoproteasome subunits. Herein, we report the syntheses, through the use of easily available protecting groups, of a variety of P1′-derivatized dihydroeponemycin analogs. We also show that certain P1′ derivatives of dihydroeponemycin irreversibly inactivate the LMP2 subunit with remarkable specificity in living cells. Finally, we show that LMP2-rich cancer cells are more sensitive to growth-inhibitory activity of the LMP2 inhibitor compared to LMP2-deficient cancer cells.

RESULTS AND DISCUSSION

Development of a Screening Assay for LMP2-Specific Compounds

Biotin-tagged epoxomicin and dihydroeponemycin [35] were used as assay probes with which to perform a screening assay for LMP2-specific compounds. We first corroborated the screening assay by western blot analysis with epoxomicin (**1**) and dihydroeponemycin (**2**), proteasome subunit-binding patterns of which have been previously well defined [31, 35]. The EL4 cell system was chosen because these cells express high levels of catalytic subunits of both the constitutive proteasome and immunoproteasomes. Specifically, various concentrations of these compounds were preincubated in EL4 cells at 37°C for 30 min. Assay probes, biotin-tagged dihydroeponemycin or epoxomicin, were then added. Cells were incubated for an additional hour at 37°C before cell lysis. Whole-cell lysates were then analyzed by using 12% SDS-PAGE and were transferred to PVDF membranes. Proteins that were newly biotinylated by assay probes were visualized by using streptavidin-horseradish peroxidase (HRP) and the enhanced chemiluminescence (ECL) detection system.

As shown in Figure 2, most of the proteasome subunit bands, which were covalently modified and visualized by using assay probes, were easily competed away with excess dihydroeponemycin, its P2 analog, or epoxomicin. This result confirms that neither epoxomicin nor dihydroeponemycin have specificity toward subunits of either the constitutive proteasome (X) or the immunoproteasome

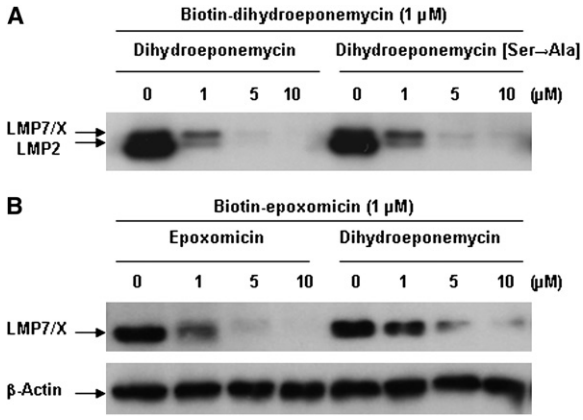

Figure 2. A Competition Assay to Test the Proteasome Subunit Binding Specificity of Proteasome Inhibitors

(A) LMP7 and X as well as LMP2 protein bands are competed away by dihydroeponemycin (**2**) or its analog (**9**) on western blot.

(B) Proteasome subunit (LMP7/X) bands are efficiently competed away by excess epoxomicin or dihydroeponemycin on western blot. EL4 cells were preincubated with proteasome inhibitors for 30 min before being treated with assay probes (biotin-epoxomicin or biotin-dihydroeponemycin). After 1 hr of incubation, cells were lysed and analyzed by western blot by using streptavidin-HRP and ECL.

(LMP2 and LMP7). Dihydroeponemycin [Ser → Ala], in which the P2 serine of the dihydroeponemycin analog is replaced with alanine, displayed a similar subunit-binding pattern to that of dihydroeponemycin. Using a similar competition assay, we screened P1′ derivatives of dihydroeponemycin for LMP2-specific compounds. Our expectation was that preincubation of a LMP2-specific inhibitor in EL4 cells will result in the modification of the threonine catalytic residue of the LMP2 subunit, preventing further modification of the occupied LMP2 subunit by assay probes. Therefore, the preoccupied LMP2 will no longer be visualized on western blot. However, proteasome catalytic subunits that are not targeted by the LMP2 inhibitor will be covalently labeled by the assay probes and visualized by western blotting by using the HRP-ECL system.

Screening Compounds that Selectively Target LMP2 in EL4 Cells

Since a linear hydrocarbon group at the P3 position is shown to provide high specificity toward the LMP2 subunit [33], the heptanoic group was positioned at the P3 site of dihydroeponemycin (Figure 1). We then focused on the derivatization at the P1′-OH group (Figure 3). First, we added an easily available methoxymethyl ether (MOM) group, preparing compounds **11** and **14**. This replacement caused a dramatic loss in the potency and specificity compared to dihydroeponemycin (Figure 4A). Similarly, compounds with a bulky *tert*-butyldiphenylsilyl (TBDPS) group (**10**) or tetrahydropyranyl (THP) group (**13**) also resulted in loss of subunit-binding activity against the immunoproteasome (Figure 4A).

Strikingly, when the MOM group was replaced with a methoxyethoxymethyl (MEM) ether group (**12**), high

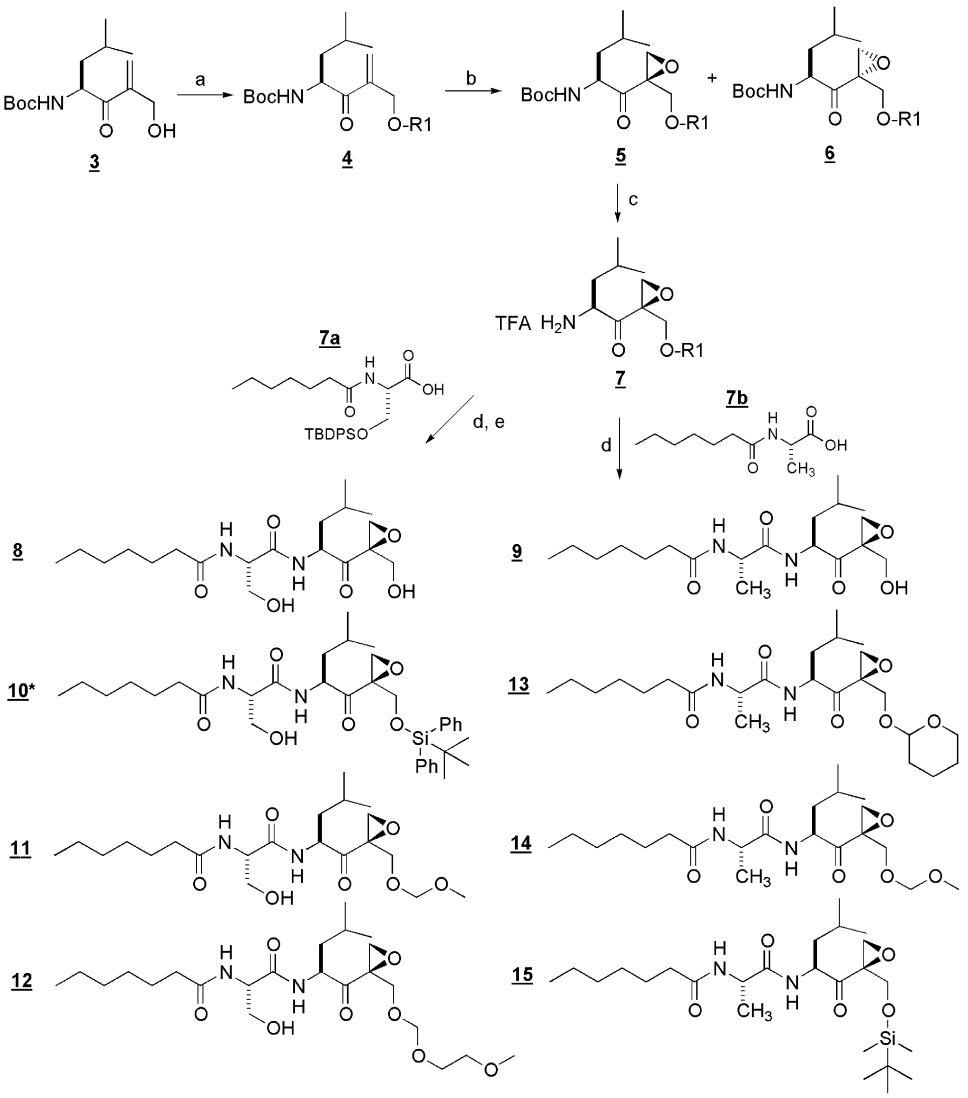

Figure 3. Synthetic Scheme of Dihydroeponemycin Analogs

Reagents and conditions for **12**. (a) 2-Methoxyethoxymethyl Chloride, *i*-Pr_2EtN, CH_2Cl_2, 0°C → rt; (b) Benzonitrile, H_2O_2, *i*-Pr_2EtN, MeOH, 0°C, 3 hr; (c) **5**, TFA, CH_2Cl_2, 30 min; (d) HBTU, HoBt, *i*-Pr_2EtN, CH_2Cl_2, rt, 12 hr; (e) TBAF, THF, 1 hr. *(e) precedes (d): **7a** was deprotected with TBAF before it was coupled to **7**.

specificity toward LMP2 was observed (Figure 4B). When a *tert*-butyldimethylsilyl (TBDMS) group was attached at the C-terminal hydroxyl group (**15**), an even higher specificity toward the LMP2 subunit was obtained, as shown in Figure 4B. Preincubation of EL4 cells with 1 μM compound **15** was sufficient to covalently modify all of the LMP2 subunit in EL4 cells, preventing further modification of the LMP2 subunit by assay probe. This resulted in selective attenuation of the LMP2 protein band on the western blot. Experiments with another assay probe (biotin-epoxomicin) (Figure 4C), which covalently labels proteasome subunits LMP7, X, MECL-1, and Z, exhibit no competition, further supporting the conclusion that both compounds **12** and **15** selectively target the LMP2 subunit, but not other proteasome subunits.

To demonstrate that compound **15** covalently and selectively modifies the LMP2 subunit, but not other subunits, we investigated the mobility shift of the LMP2-**15** adduct by using EL4 cells (Figure 4D). After EL4 cells were incubated with compound **15** or assay probes (biotinylated epoxomicin [Biotin-EPX] and Biotin-EPN) for 1.5 hr at 37°C, cells were lysed. Whole-cell proteins were then analyzed by western blot with anti-LMP2, anti-LMP7, anti-X, and anti-Y antibodies. In this experiment, biotinylated epoxomicin (Biotin-EPX) and biotinylated dihydroeponemycin (Biotin-EPN) were used as mobility shift controls since they have been shown to cause mobility shift via covalent modification of LMP2 [31, 32, 36].

Due to increased molecular weights (by 828.08 for biotin-epoxomicin and 1078.45 for biotin-dihydroeponemycin),

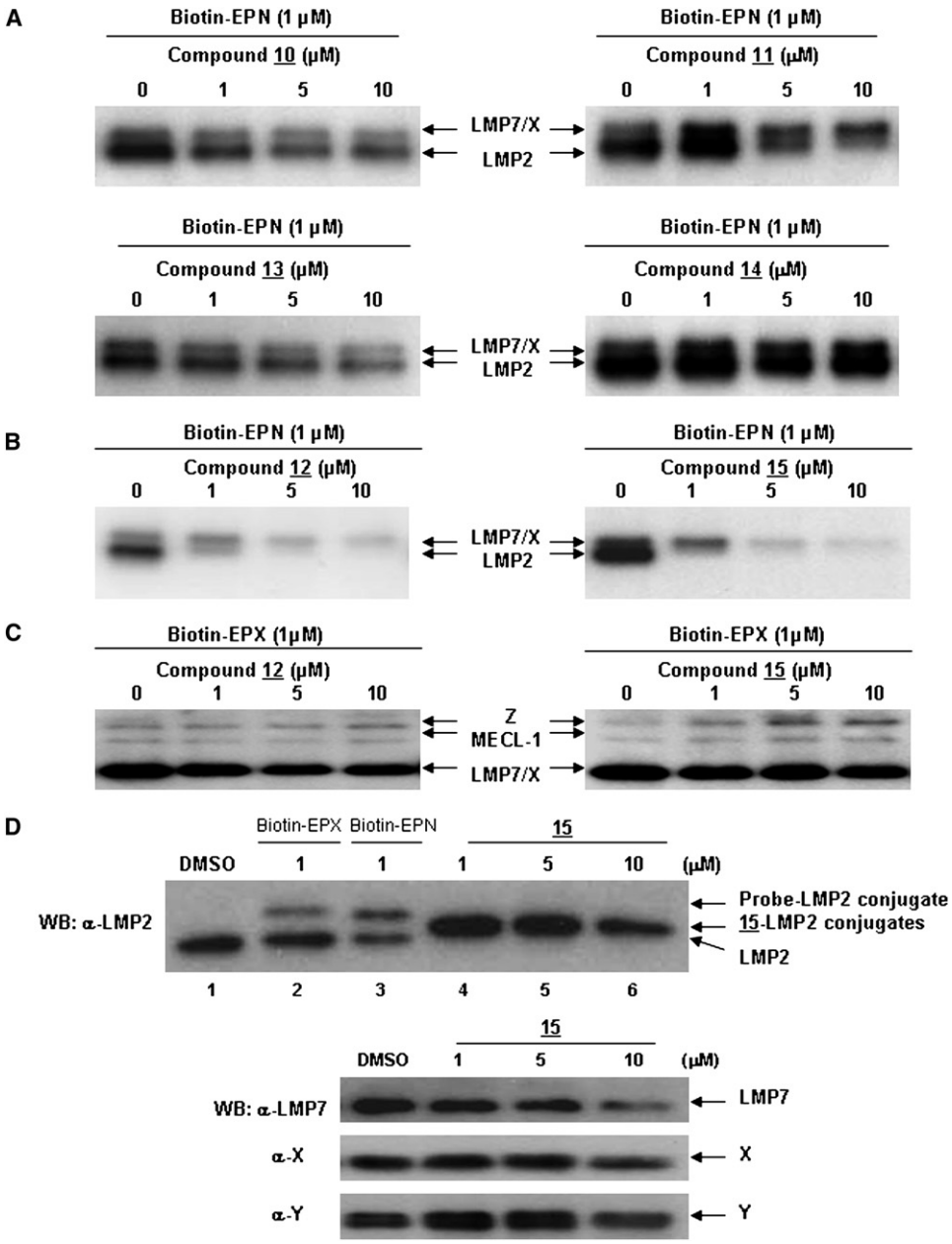

Figure 4. Proteasome Subunit LMP2-Specific Binding by Two Eponemycin Analogs

(A–C) EL4 cells were preincubated with compounds before the treatment of assay probes for visualization of proteasome subunits that are not targeted by compounds **12** and **15**. (A) Compounds **10**, **11**, and **13** nonselectively target proteasome subunits, whereas compound **14** does not bind proteasome subunits. (B) Compounds **12** and **15** selectively target the immunoproteasome subunit LMP2. (C) Compounds **12** and **15** do not target other catalytic subunits (LMP7, X, Z, and MECL1).

(D) Cells were incubated for 1 hr before SDS-PAGE and western blot analysis with anti-LMP7, X, and Y antibodies. Compound **15** covalently modifies the immunoproteasome subunit LMP2, but not other subunits in EL4 cells.

Biotin-EPN, Biotinylated dihydroeponemycin; Biotin-EPX, Biotinylated epoxomicin.

assay probe-LMP2 adducts displayed a slower mobility shift when compared to free LMP2 (lanes 1–3, Figure 4D). While a mobility shift for the LMP2-**15** adduct on SDS-PAGE was clearly shown in comparison to free LMP2 (lanes 4–6, Figure 4D), it was observed to be slower than that of assay probe-LMP2 adducts (lanes 2–3 versus lanes 4–6). This can be explained with the lower molecular weight of compound **15** (484.76) as compared to the assay probes. While 1 μM compound **15**, but not the assay probes, was sufficient to modify most of the LMP2 subunits in cells (lanes 2–3 versus 4–6), no mobility shift was observed in other proteasome subunits, indicating that

compound **15** selectively inactivates the LMP2 subunit with high efficiency.

Compound 15 Blocks Chymotrypsin-like Activity of the LMP2 Subunit but Has No Effect on the Activity of the Constitutive Proteasome in an Angiogenesis Cell Model

The elucidation of protein function, especially with regard to multiprotein complexes, is clearly one of the important goals of the small-molecule approach to cell biology. With respect to the proteasomal complex, researchers have long been interested in assigning specific catalytic activities to each β subunit of the proteasome. Based on data obtained from X-ray analysis and direct inhibition of proteasome activities with a variety of proteasome inhibitors, all three β subunits of the constitutive proteasome have been assigned to three different activities [4, 9, 37, 38]. Whereas LMP7 and MECL1 of the immunoproteasome are shown to possess CT-L and T-L activities, respectively, a clear assignment for the LMP2 subunit of the immunoproteasome has not yet been made. LMP2, which replaces the constitutive proteasome catalytic subunit Y that is responsible for C-L activity, has been suggested to cleave substrates after hydrophobic amino acid residues to generate peptides favored for MHC class I presentation [39, 40], but experimental data to support this assumption are lacking. Therefore, with our LMP2-specific inhibitor in hand, we wanted to determine whether LMP2 is responsible for CT-L activity. To test this, we used the natural product lactacystin, which primarily binds the LMP7 (and MECL1) subunit [41] and inactivates its catalytic activity [42, 43], and then determined whether free LMP2 has CT-L activity. It should be noted that MECL1 is reported to be responsible for T-L activity [44, 45]. As shown in Figure 5A, when the immunoproteasome was preincubated with lactacystin at the concentration at which 95% of the CT-L activity of the constitutive proteasome is inhibited, ~20% of the CT-L activity of the immunoproteasome was blocked compared to control. Similarly, when the immunoproteasome was preincubated with compound **15** at the concentration at which only LMP2 is inactivated (see Figures 4D and 6D), ~20% of the CT-L activity of the immunoproteasome was also inhibited (Figure 5A). In the presence of both lactacystin and compound **15**, ~45% of the CT-L activity was blocked, whereas the CT-L activity of the immunoproteasome was completely blocked when the concentration of either lactacystin or compound **15** was increased (data not shown). This finding indicates that these compounds have an additive inhibitory action on the CT-L enzymatic function of the immunoproteasome. Collectively, these results suggest that LMP2 is, at least in part, responsible for the CT-L activity of the immunoproteasome.

Despite the fact that compound **15** selectively modifies the catalytic LMP2 subunit and inhibits the CT-L activity of the immunoproteasome, it is still unclear whether compound **15** also inhibits essential CT-L activity of the constitutive proteasome in living cells. Thus, we next tested whether compound **15** can disrupt cellular events that are regulated by the constitutive proteasome. Angiogenic growth of blood vessels requires normal activities of the constitutive proteasome and is highly sensitive to proteasome inhibitors [46] such as epoxomicin and dihydroeponemycin. Conversely, endothelial cells do not normally express the immunoproteasome (data not shown), and, thus, we expect that angiogenic sprouting in an in vitro model will be highly sensitive to regular proteasome inhibitors, but not to LMP2-specific inhibitors.

The three-dimensional endothelial cell sprouting assay (3D-ECSA) is an in vitro experimental system that closely mimics the in vivo angiogenesis processes, featuring the differentiation of endothelial cells into sprouting structures within a 3D matrix of fibrin or collagen I [47]. We employed the 3D-ECSA assay to investigate whether compound **15** and proteasome inhibitors differ in their inhibitory activity on growth factor-induced sprouting angiogenesis. As anticipated, epoxomicin [2] and dihydroeponemycin potently inhibited sprouting morphogenesis due to inhibition of the essential constitutive proteasome activity (Figure 5B). On the other hand, compound **15** did not inhibit endothelial sprouting at doses much higher than those of dihydroeponemycin or epoxomicin, even though compound **15** is more efficient at inactivating the LMP2 subunit (see Figure 4D). Quantitative measurements of endothelial sprouting as described earlier [46, 48] revealed that compound **15** with concentration as high as 10 μM only marginally disrupts sprouting (~80-fold higher concentration than dihydroeponemycin) (data not shown). Similarly, compound **12** did not inhibit endothelial sprouting. These angiogenesis assay results indicate that the LMP2 inhibitors do not perturb the functions of the constitutive proteasome in living cells.

LMP2-Specific Inhibitors Selectively and Covalently Inactivate the LMP2 Subunit in PC3 Prostate Cancer Cells

Given that one of our goals is to explore the pathophysiological functions of LMP2 in relevant disease models, we questioned whether LMP2 inhibitors developed here have any impact on normal biological processes of cancer cells that predominantly express LMP2. First, we investigated which prostate cancer cells constitutively express the LMP2 subunit. Surprisingly, among the prostate cancer cell lines examined, only androgen-independent PC3 prostate cancer cells, but not androgen-dependent LNCaP or LN3 cells, constitutively expressed the immunoproteasome catalytic subunit LMP2 (Figure 6A). Remarkably, the specificity of compounds **15** and **12** toward LMP2 is even more evident in PC3 cells compared to EL4 cells. As shown in Figure 6B, the LMP2 protein band in PC3 cells was selectively attenuated by the LMP2 inactivators **15** and **12**, indicating their high specificity toward the LMP2 subunit. Unlike epoxomicin or dihydroeponemycin, compounds **12** and **15** did not compete with the biotinylated probes for binding of LMP7, X, Z, and MECL1 (Figure 6C). Mobility shift assays with western blot, which is analyzed with anti-LMP2, -LMP7, -X, or -Y antibodies, clearly showed that compound **15** covalently

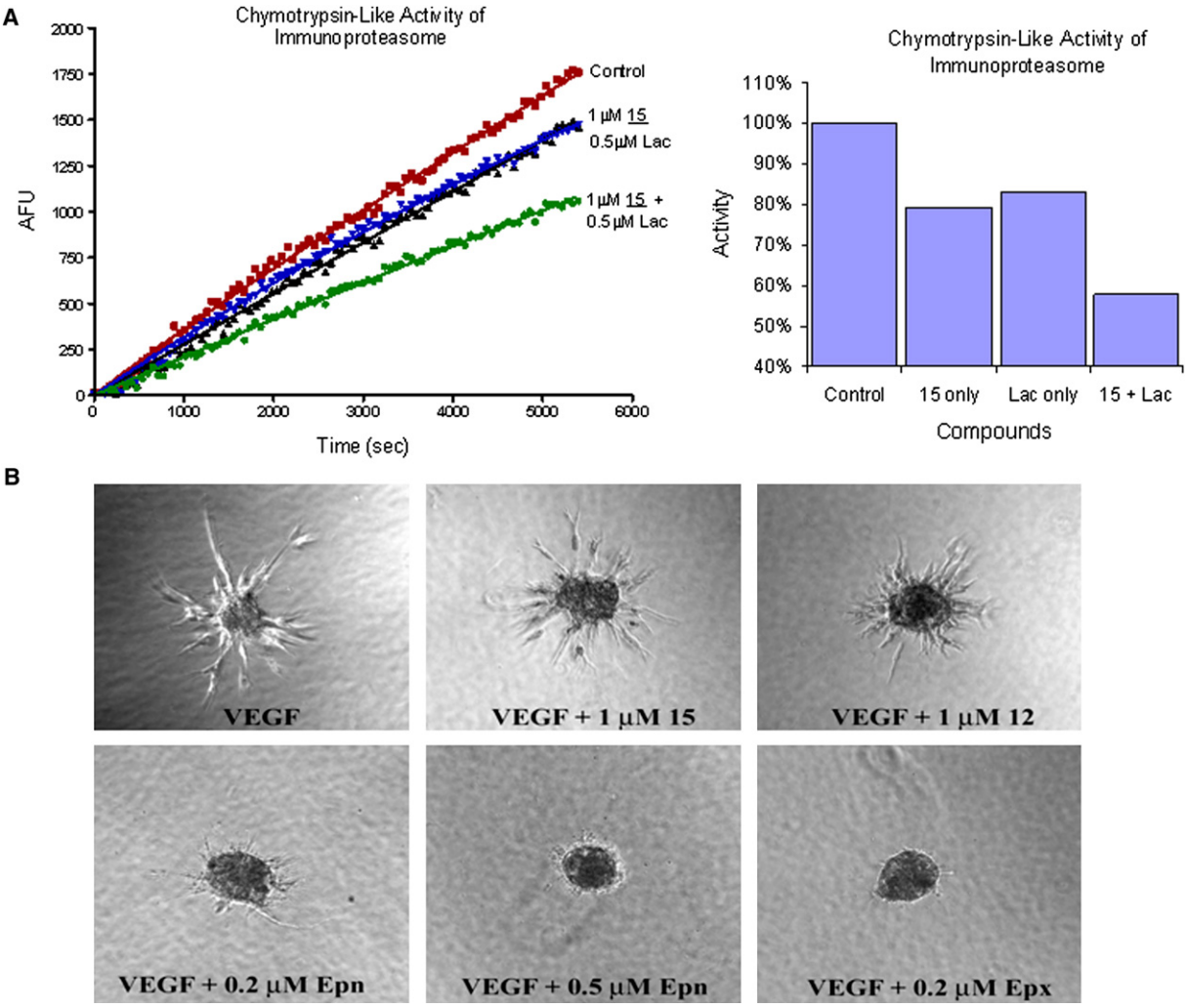

Figure 5. Inhibition of Chymotrypsin-like Activity of the Immunoproteasome by Compound 15

(A) Inhibition of chymotrypsin-like activity of the immunoproteasomes by compound **15**. Proteasome kinetic studies were performed with purified immunoproteasome. Purified immunoproteasome was preincubated with lactacystin, compound **15**, or cotreatment for 30 min before CT-L fluorogenic substrate was added (Suc-Leu-Leu-Val-Tyr-AMC). Data were collected over a 1.5 hr period at room temperature. For compound **15**, $K_{obs}/[I]$ ($M^{-1}S^{-1}$) = 83 ± 27. The range of inhibitor concentrations used was 5–20 μM.

(B) Compounds **15** and **12** do not inhibit the constitutive proteasome. Human endothelial cell spheroids were seeded in collagen I gels in a 96-well plate and were stimulated with vascular endothelial growth factor (VEGF; 20 ng/ml) to induce angiogenic sprouting. In replicate wells, VEGF-treated spheroids were coincubated with epoxomicin (Epox), dihydroeponemycin (Epn), compound **15**, or compound **12**. Representative photographic images of spheroids taken after 24 hr show invasive growth of vessel structures with VEGF alone and compound **15** cotreatment or compound **12** cotreatment, but a potent inhibitory effect with dihydroeponemycin (0.2 μM and 0.5 μM) or epoxomicin (0.2 μM) cotreatment.

inactivates LMP2, but not the other catalytic subunits of proteasomes (Figure 6D). Similar to the results obtained from the mobility shift experiments with EL4 cells (Figure 4D), compound **15** was a more potent LMP2 inhibitor than the biotinylated probes. Probe-LMP2 conjugates at 1 μM concentration were not even observed in the western blot experiments (lanes 2 and 3 in Figure 6D). LMP7, X, and Y subunits were not covalently modified by compound **15** even at 10 μM concentration. These results clearly indicate that compound **15** selectively modifies LMP2 constitutively expressed in PC3 prostate cancer cells.

LMP2-Rich PC3 Prostate Cancer Cells Are More Sensitive to Growth-Inhibitory Activity of the LMP2-Specific Inhibitor than LMP2-Deficient Prostate Cancer Cells

Next, we wished to determine whether the LMP2-specific inhibitor has effects on the proliferation of PC3 cancer cells that highly express LMP2. Given that LMP2 is a major catalytic subunit of the immunoproteasome and the fact that proteasomes play an important role in cell growth, we hypothesized that PC3 cells may be more sensitive to the LMP2 inhibitor **15** compared to LMP2-deficient LN3 prostate cancer cells. In contrast, we expect that

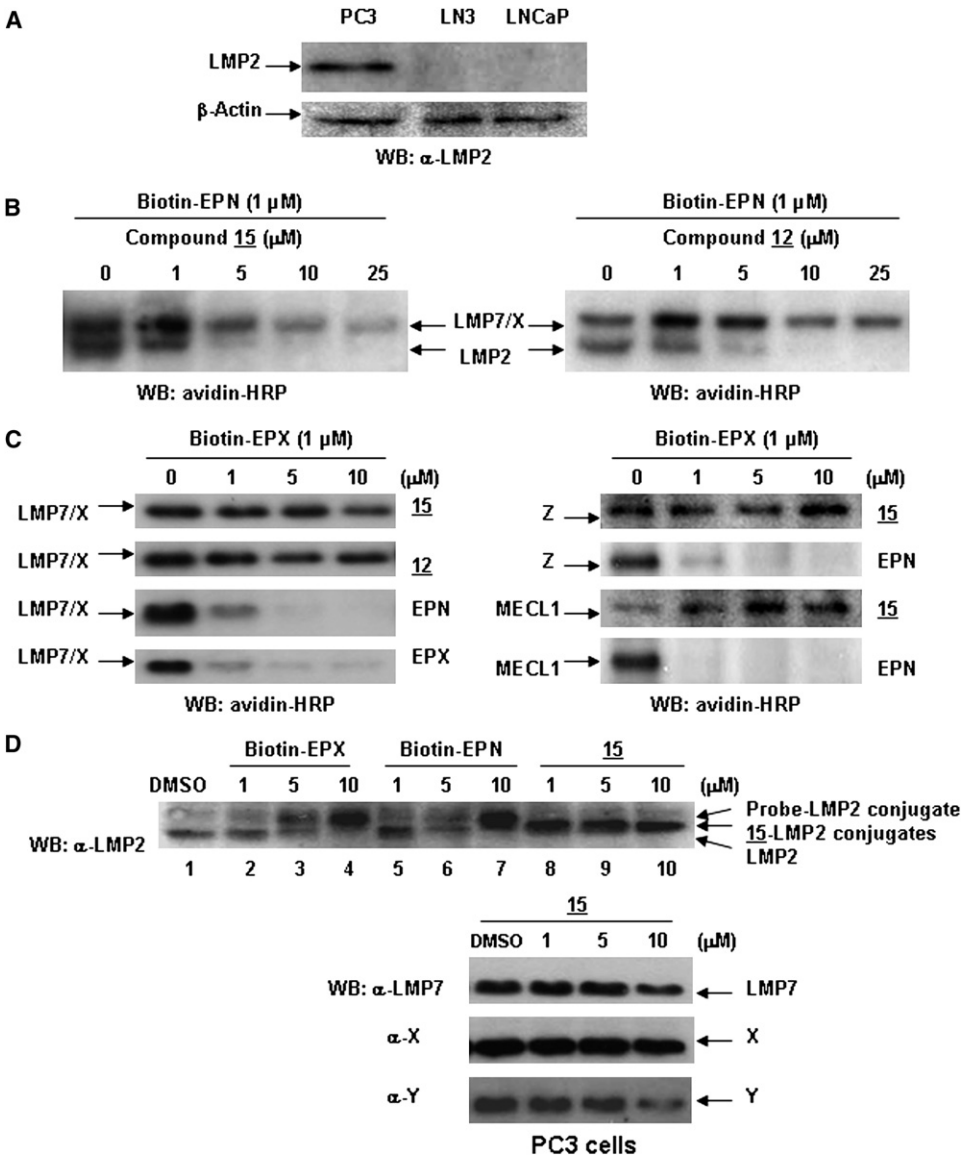

Figure 6. Selective Modification of the LMP2 Subunit in PC3 Prostate Cancer Cells

(A) LMP2 expression levels of prostate cancer cells.

(B and C) PC3 cells were preincubated with compounds before the treatment of biotinylated dihydroeponemycin to visualize biotinylated proteasome subunits that are not targeted by compounds **12** and **15**. (B) Compounds **12** and **15** selectively target the immunoproteasome subunit LMP2 in PC3 prostate cancer cells. (C) Compounds **12** and **15** do not compete with epoxomicin or dihydroeponemycin for binding Z, MECL1, LMP7, and X subunits.

(D) Compound **15** covalently modifies the immunoproteasome subunit LMP2 in PC3 prostate cancer cells. Cells were incubated with compound **15**, biotin-epoxomicin, or biotin-dihydroeponemycin for 1.5 hr. The mobility shift of the LMP2 subunit was analyzed by western blotting with anti-LMP2 antibody.

DPN, dihydroeponemycin; EPX, epoxomicin.

the broadly acting proteasome inhibitors epoxomicin and dihydroeponemycin will not display differential activity toward the prostate cancer cells regardless of their expression level of LMP2. We tested this hypothesis by measuring IC_{50} values for compound **15** in both PC3 (LMP2-positive) and LN3 (LMP2-deficient) cells. Remarkably, PC3 cells are about 7-fold more sensitive to the LMP2 inhibitor **15** than LN3 prostate cancer cells (Table 1). In contrast, both PC3 and LN3 cells were similarly sensitive to the broad-spectrum proteasome inhibitors epoxomicin and dihydroeponemycin.

Although it is currently not clear why PC3 cancer cells, but not other prostate cancer cell lines, constitutively express LMP2, these results indicate that LMP2 may play an important role in proliferation of cancer cells that constitutively express LMP2. It is also not known whether

Table 1. Trypan Blue Exclusion Assays Were Performed by Counting Cell Numbers after 48 hr of Incubation with Compound 15 or the Random Proteasome Inhibitors Dihydroeponemycin and Epoxomicin

	IC_{50} (μM)[a]		Relative Sensitivity[b]
Cell line	LN3	PC3	-
LMP2 expression	No	Yes	-
15	14.34	2.04	~7
Dihydroeponemycin	0.49	0.36	1
Epoxomicin	0.015	0.009	1

[a] Experiments were repeated at least three times or more.
[b] Relative sensitivity of LMP2-positive PC3 cells to inhibitors compared to the LMP2-deficient LN3 cell line = $IC_{50}^{LN3}/IC_{50}^{PC3}$.

LMP2 within the immunoproteasome or monomeric LMP2 is a pharmacological target of compound **15**. Although it is presumed that newly synthesized LMP2 (pre-LMP2) is catalytically inactive until it has matured into catalytically active LMP2 by LMP7 and has been assembled into the immunoproteasome [49–51], the possibility of alternative maturation into a catalytically active LMP2 monomer that may be functionally important in cell proliferation cannot be ruled out. Regardless, the high sensitivity of LMP2-rich PC3 cancer cells to compound **15** suggests that LMP2 may be a target for therapeutic intervention in cancers that constitutively express this protein. Additionally, these findings have allowed us to conclude that compound **15** may be a molecular probe of LMP2 function that can be exploited to illuminate the biological roles of its substrates in immunoproteasome-dependent processes.

In conclusion, we have developed an epoxyketone-pharmacophore-based LMP2-specific probe with which the physiological roles of LMP2 in cells can be investigated. As the LMP2 inhibitor blocks proliferation of LMP2-rich cancer cells with high specificity, it can now be utilized to determine whether the LMP2 subunit is a valid target for therapeutic intervention in animal models of cancer. Further, compound **15** can also be used as a chemical knockout reagent of LMP2 to screen for immunoproteasome substrates that are distinct from regular proteasome substrates, which will ultimately enhance our understanding of the role of LMP2 in pathogenic diseases.

SIGNIFICANCE

The immunoproteasome catalytic subunits have been implicated in a number of disease states. For example, they have been suggested as potential new drug discovery targets for the treatment of multiple myeloma. However, there are currently no immunoproteasome catalytic subunit-specific inhibitors that can be used to validate these subunits as therapeutic targets. Furthermore, the exact role of the immunoproteasome catalytic subunits in pathogenesis is not clearly understood. Thus, the development of the immunoproteasome catalytic subunit LMP2-specific inhibitors described in this report may not only hold great potential as a therapeutic agent for certain diseases, but can also provide a valuable chemical genetic probe to investigate immunoproteasome biology.

EXPERIMENTAL PROCEDURES

General Remark

Unless otherwise stated, all reactions were carried out under nitrogen with dry, freshly distilled solvents, oven-dried glassware, and magnetic stirring. All solvents were reagent grade. Tetrahydrofuran (THF) was distilled from sodium/benzophenone. Methylene chloride (CH_2Cl_2) was distilled from calcium hydride. Diethyl ether anhydrous was purchased from EMD Chemicals and was used without further purification. All reagents were purchased from Sigma-Aldrich and were used without further purification. All reactions were monitored by thin-layer chromatography (TLC) by using E. Merk $60F_{254}$ precoated silica gel plates. Flash column chromatography was performed by using E. Merk silica gel 60 (particle size 0.040–0.063 mm) and was performed with the indicated solvents. ^1H was recorded in $CDCl_3$ by using a Varian 300MHz spectrometer at ambient temperature with an internal deuterium lock unless stated otherwise. Chemical shifts are referenced to residual chloroform (δ = 7.27 ppm for ^1H). High- and low-resolution mass spectra were carried out by the University of Kentucky Mass Spectrometry Facility.

Synthesis of **12** is described here as the representative synthetic procedure for dihydroeponemycin analogs.

(4*S*)-4-(*tert*-Butoxycarbonyl)-Amino-2-Hydroxy-Methyl-6-Methylhept-1-En-3-One, 3

Synthetic procedures were performed as previously reported [11].

(4*S*)-4-(*tert*-Butoxycarbonyl)-Amino-2-(Methoxy-Ethoxymethoxymethyl)-6-Methylhept-1-En-3-One, 4

Methoxyethoxymethyl chloride (0.24 ml, 2.1 mmol) and diisopropylethylamine (0.37 ml, 2.1 mmol) were added to a solution of **3** (114 mg, 0.42 mmol) in CH_2Cl_2 (5 ml) at 0°C. After stirring at room temperature for 3 hr, the resulting mixture was poured into ice water (20 ml) and extracted with CH_2Cl_2 (3 × 20 ml). The organic layers were combined, washed with brine (20 ml), dried with Na_2SO_4, filtered, and concentrated under reduced pressure. The product was then subjected to flash column chromatography (5:1 hexane:EtOAc), yielding **4** (101 mg, 67%) as a yellowish oil. ^1H NMR: δ = 6.20 (d, ^2J = 31.8 Hz, 2H, 1-H), 5.12 (d, ^2J = 9.0 Hz, 1H, N*H*), 5.03 (m, 1H, 4-H), 4.75 (s, 2H, 2-OCH_2O), 4.28 (s, 2H, 2-CH_2), 3.69 (m, 2H, 2-OCH_2CH_2O), 3.55 (m, 2H, 2-OCH_2CH_2O), 3.38 (s, 3H, 2-OCH_3), 1.74 (m, 1H, 6-H), 1.50 (m, 1H, 5-H^a), 1.41 (s, 9H, H_{Boc}), 1.31 (m, 1H, 5-H^b), 0.99 (d, ^3J = 6.6 Hz, 3H, CH_3CHCH$_3$), 0.90 (d, ^3J = 6.6 Hz, 3H, CH$_3$CHCH_3) ppm.

(2*RS*,4*S*)-4-(*tert*-Butoxycarbonyl)-Amino-2-(Methoxy-Ethoxymethoxymethyl)-6-Methyl-1,2-Oxiranyl-Heptane, 5 and 6

Benzonitrile (0.29 ml, 2.8 mmol), H_2O_2 (0.40 ml, 50% solution in H_2O, 7.0 mmol), and diisopropylethylamine (0.5 ml, 2.8 mmol) were added to a solution of **4** (100 mg, 0.28 mmol) in MeOH (5 ml) at 0°C. The reaction was stirred at 0°C for 3 hr. The resulting mixture was then concentrated under reduced pressured and was subjected to flash column chromatography (10:1 hexane:EtOAc) to yield **5** and **6** at a ratio of 3:1 (60 mg, 60%). **5**: ^1H NMR: δ = 4.82 (d, ^2J = 8.4 Hz, 1H, N*H*), 4.71 (s, 2H, 2-OCH_2O), 4.39 (d, ^2J = 11.4 Hz, 1H, 2-CH^a_2), 4.32 (m, 1H, 4-H), 3.68 (m, 2H, 2-OCH_2CH$_2$O), 3.57 (m, 2H, 2-OCH$_2$CH_2O), 3.49 (d, ^2J = 11.4 Hz, 1H, 2-CH^b_2), 3.40 (s, 3H, 2-OCH_3), 3.27 (d, ^2J = 4.8 Hz, 1H, 1-H^a), 3.03 (d, ^2J = 4.8 Hz, 1H, 1-H^b), 1.75 (m, 1H, 6-H),

1.58 (m, 1H, 5-H^a), 1.41 (s, 9H, H_{Boc}), 1.13 (m, 1H, 5-H^b), 0.97 (d, ^3J = 6.6 Hz, 3H, CH_3CHCH_3), 0.94 (d, ^3J = 6.6 Hz, 3H, CH_3CHCH_3) ppm.

(*S*)-*O*-*tert*-Butyldiphenylsiloxymethyl-*N*-Heptanoyl-Serine, 7

Lithium hydroxide (91 mg, 3.8 mmol) was added to a solution of (*S*)-*O*-*tert*-butyldiphenyl-siloxymethyl-*N*-heptanoyl-seryl methyl ester (890 mg, 1.8 mmol) in a methanol:water (3:1) solution. The reaction was stirred at 5°C for 15 hr. The resulting mixture was poured into H_2O with cold 1 N HCl and was extracted with CH_2Cl_2. The organic layers were combined, washed with brine, dried under Na_2SO_4, filtered, concentrated, and dried under high vacuum. The product obtained yielded **7** as a yellowish oil. ^{1}H NMR: δ = 7.61 (m, 4H, Ar-H), 7.41 (m, 6H, Ar-H), 6.24 (d, ^2J = 7.5 Hz, 1H, N*H*), 4.69 (m, 1H, 2-H), 4.17 (dd, ^2J = 10.4 Hz, ^2J = 3.6 Hz, 1H, 3-H^a), 3.89 (dd, ^2J = 10.4 Hz, ^2J = 3.6 Hz, 1H, 3-H^b), 2.20 (t, ^3J = 7.5 Hz, 2H, 2′-H), 1.60 (m, 2H, H_{Hep}), 1.29 (m, 6H, H_{Hep}), 1.05 (s, 9H, H_{butyl}), 0.88 (t, ^3J = 6.9 Hz, 3H, 7′-CH_3) ppm.

(*S*)-*O*-*tert*-Butyldiphenylsiloxymethyl-*N*-Heptanoyl-Seryl Methyl Ester

tert-butyldiphenylsilyl chloride (1.95 ml, 7.6 mmol) and imidazole (519 mg, 7.6 mmol) were added to a solution of (*S*)-*N*-heptanoyl-serine methyl ester (588.6 mg, 2.5 mmol) in CH_2Cl_2 (20 ml), and the solution was stirred overnight at room temperature. The resulting mixture was concentrated under reduced pressure and was subjected to column chromatography (5:1 hexane:EtOAc), yielding (*S*)-*O*-*tert*-butyldiphenylsiloxymethyl-*N*-heptanoyl-seryl methyl ester (890 mg, 74%) as a colorless oil. ^{1}H NMR: δ = 7.59 (m, 4H, Ar-H), 7.41 (m, 6H, Ar-H), 6.28 (d, ^2J = 8.4 Hz, 1H, N*H*), 4.70 (m, 1H, 2-H), 4.12 (dd, ^2J = 10.1 Hz, ^2J = 3.0 Hz, 1H, 3- H^a), 3.89 (dd, ^2J = 10.1 Hz, ^2J = 3.0 Hz, 1H, 3-H^b), 3.74 (s, 3H, 1-OCH_3), 2.11 (t, ^3J = 7.7 Hz, 2H, 2′-H), 1.57 (m, 2H, H_{Hep}), 1.30 (m, 6H, H_{Hep}), 1.04 (s, 9H, H_{butyl}), 0.88 (t, ^3J = 6.7 Hz, 3H, 7′-CH_3) ppm.

(*S*)-*N*-Heptanoyl-Serine Methyl Ester

HBTU (1.83 g, 4.8 mmol), HOBt (0.74 g, 4.8 mmol), and lastly diisopropylethylamine (2.8 ml, 16 mmol) were added to a solution of heptanoic acid (0.46 ml, 3.2 mmol) and H-Ser-OCH_3 (0.5 g, 3.2 mmol) in CH_2Cl_2 (15 ml). The reaction was stirred overnight at room temperature. The resulting mixture was subjected to flash column chromatography (1:2 hexane:EtOAc), yielding (*S*)-*N*-heptanoyl-serine methyl ester (588.6 mg, 79%) as a yellowish oil. ^{1}H NMR: δ = 6.47 (b, 1H, N*H*), 4.69 (m, 1H, 2-H), 3.94 (m, 2H, 3-H), 3.79 (s, 3H, 1-OCH_3), 2.27 (t, ^3J = 7.6 Hz, 2H, 2′-H), 1.63 (m, 2H, H_{Hep}), 1.29 (m, 6H, H_{Hep}), 0.88 (m, 3H, 7′- CH_3) ppm.

(4*S*)-2-Methoxyethoxy-Methoxymethyl-4-([*S*]-*O*-*tert*-Butyldiphenylsiloxy-Methyl-*N*-Heptanoylseryl-Amino)-6-Methyl-1,2-Oxiranyl-Heptane

Trifluoroacetic acid (100 μl, 0.87 mmol) was added to a solution of **5** (45 mg, 0.12 mmol) in CH_2Cl_2 (0.5 ml) at room temperature for 30 min. Subsequently, the concentrated mixture was dried under high vacuum to remove trifluoroacetic acid. The resulting crude product, **6** (33 mg, ca. 100%), was then used in the following coupling reaction without further purification. HBTU (68 mg, 0.17 mmol), HOBt (27 mg, 0.17 mmol), and lastly diisopropylethylamine (104 μl, 0.59 mmol) were added to a solution of **6** (33 mg, 0.12 mmol) and **7** (65 mg, 0.14 mmol) in CH_2Cl_2 (5 ml). The reaction was stirred overnight at room temperature. The resulting mixture was subjected to flash column chromatography (3:1 hexane:EtOAc) to give (4*S*)-2-methoxyethoxy-methoxymethyl-4-([*S*]-*O*-*tert*-butyldiphenylsiloxy-methyl-*N*-heptanoylseryl-amino)-6-methyl-1,2-oxiranyl-heptane (36 mg, 42%). ^{1}H NMR: δ = 7.71 (m, 4H, Ar-H), 7.44 (m, 6H, Ar-H), 7.02 (d, ^2J = 8.4 Hz, 1H, 4-N*H*), 6.17 (d, ^2J = 6.6 Hz, 1H, 2′-N*H*), 4.72 (s, 2H, 2-OCH_2O), 4.60 (m, 2H, 4-H, 2′-H), 4.42 (d, ^2J = 11.4 Hz, 1H, 2-CH^a_2), 4.03 (m, 1H, 3′-H^a), 3.70 (m, 3H, 3′-CH^b_2, 2-OCH_2CH_2O), 3.55 (m, 2H, 2-OCH_2CH_2O), 3.52 (d, ^2J = 11.4 Hz, 1H, 2-CH^b_2), 3.40 (s, 3H, 2-OCH_3), 3.29 (d, ^2J = 5.4 Hz, 1H, 1-H^a), 3.04 (d, ^2J = 4.8 Hz, 1H, 1-H^b), 2.13 (t, ^3J = 7.6 Hz, 2H, 2″-H), 1.63 (m, 4H, 6-H, 5-H^a, H_{Hep}), 1.26 (m, 6H, H_{Hep}), 1.07 (s, 9H, 3′-*t*Bu), 0.96 (d, ^3J = 6.3 Hz, 3H, CH_3CHCH_3), 0.91 (d, ^3J = 6.3 Hz, 3H, CH_3CHCH_3), 0.86 (t, ^3J = 7.6 Hz, 3H, 7″- CH_3) ppm.

(4*S*)-2-Methoxyethoxymethoxymethyl-4-*N*-Heptanoylserylamino-6-Methyl-1,2-Oxiranylheptane, 12

Tetrabutylammonium fluoride (50 μl, 1 M in THF, 0.05 mmol) was added to a solution of (4*S*)-2-methoxyethoxy-methoxymethyl-4-([*S*]-*O*-*tert*-butyldiphenylsiloxy-methyl-*N*-heptanoylseryl-amino)-6-methyl-1,2-oxiranyl-heptane (30 mg, 0.042 mmol) in THF (1 ml). The reaction was stirred at room temperature for 1 hr, followed by flash column chromatography (1:2 hexane:EtOAc), yielding **12** (16 mg, 80%) as a yellowish oil. ^{1}H NMR: δ = 6.83 (d, ^2J = 7.5 Hz, 1H, 4-N*H*), 6.44 (d, ^2J = 7.5 Hz, 1H, 2′-N*H*), 4.71 (s, 2H, 2-OCH_2O), 4.50 (m, 2H, 4-H, 2′-H), 4.41 (d, ^2J = 11.7 Hz, 1H, 2-CH^a_2), 4.08 (m, 1H, 3′-H^a_2), 3.68 (m, 2H, 2-OCH_2CH_2O), 3.55 (m, 3H, 2-OCH_2CH_2O, 3′-H^b_2), 3.46 (d, ^2J = 11.7 Hz, 1H, 2-CH^b_2), 3.40 (s, 3H, 2-OCH_3), 3.27 (d, ^2J = 5.1 Hz, 1H, 1-H^a), 3.05 (d, ^2J = 4.8 Hz, 1H, 1-H^b), 2.22 (m, 2H, 2″-H), 1.60 (m, 4H, 6-H, 5-H^a, H_{Hep}), 1.28 (m, 6H, H_{Hep}), 0.96 (d, ^3J = 3.9 Hz, 3H, CH_3CHCH_3), 0.94 (d, ^3J = 3.9 Hz, 3H, CH_3CHCH_3), 0.88 (t, ^3J = 6.7 Hz, 3H, 7″- CH_3) ppm. MS (ESI): m/z = 475, calcd. for $C_{23}H_{42}N_2O_8$: m/z = 474.59.

Cell Culture and Screening Assay

Murine lymphoma EL4 cells and prostate cancer PC3 cells (ATCC) were grown in RPMI medium (GIBCO-BRL) supplemented with 10% fetal bovine serum and 1% penicillin and streptomycin at 37°C in a 5% CO_2 incubator. Cells were pretreated with 1 μM biotinylated compounds 30 min prior to the addition of increasing concentrations of either dihydroeponemycin, epoxomicin, or dihydroeponemycin analogs as indicated. The cells were then incubated for an additional hour. Cell lysates were analyzed by 12% SDS-PAGE and were transferred to PVDF membranes. Proteins that were covalently modified by biotinylated compounds were visualized with enhanced chemiluminescence by using streptavidin-conjugated horseradish peroxidase (Sigma-Aldrich) or anti-LMP2 (Affinity BioReagents) and Biomax X-ray film (Kodak).

Enzyme Kinetic Studies

k association values were determined as follows. Inhibitors were mixed with a fluorogenic peptide substrate and assay buffer (20 mM Tris [pH 8.0], 0.5 mM EDTA, and 0.035% SDS) in a 96-well plate. The chymotrypsin-like activity was assayed by using the fluorogenic peptide substrates Suc-Leu-Leu-Val-Tyr-AMC (Sigma-Aldrich). Hydrolysis was initiated by the addition of bovine 20S proteasome or immunoproteasome (Biomol International), and the reaction was followed by fluorescence (360 nm excitation/460 nm detection) by using a Microplate Fluorescence Reader (FL600; Bio-Tek Instruments, Inc., Winooski, VT) employing the software KC4 v.2.5 (Bio-Tek Instruments, Inc.). Reactions were allowed to proceed for 60–90 min, and fluorescence data were collected every 1 min. Fluorescence was quantified as arbitrary units, and progression curves were plotted for each reaction as a function of time. $k_{observed}$/[I] values were obtained by using the PRISM program by nonlinear least-squares fit of the data to the following equation: $\text{fluorescence} = v_s t + ([v_0 - v_s]/k_{observed})(1 - \exp[-k_{observed}\, t])$, where v_0 and v_s are the initial and final velocities, respectively, and $k_{observed}$ is the reaction rate constant. The range of inhibitor concentrations tested was chosen so that several half-lives could be observed during the course of the measurement. Reactions were performed with inhibitor concentrations that were < 100-fold of those of the proteasome assayed.

3D-Endothelial Cell Sprouting Assay, 3D-ECSA

Endothelial cell spheroids were generated from human umbilical vein endothelial cells (HUVECs; Cascade Biologicals, Portland, OR) as described [48]. The spheroids (4–6/well) were distributed in 96-well plates in collagen I matrix for the 3D-ECSA. Cell culture medium was added to each well along with 20 ng/ml VEGF in the presence and absence of the individual inhibitor. The 3D cultures were incubated in tissue

culture chambers at 37°C in 5% CO_2 for 24 hr. Photographic images of spheroids were obtained with the 10× objective of a Nikon TE2000 microscope. Sprouting was quantified from digital images according to our previously published method [46].

Trypan Blue Exclusion Assay

Prostate cancer PC3 and LN3 cells were seeded in 12-well plates. They were then incubated at 37°C until they were 70% confluent before the appropriate inhibitors were added as indicated in increasing concentrations. Cells were treated for 48 hr. Viable cells were counted on a hemocytometer in 0.2% trypan blue solution (Sigma-Aldrich). IC_{50} values were calculated from sigmoid dose-response curves by the method of nonlinear regression to a logarithmic function. These data represent the average of three or more experiments.

ACKNOWLEDGMENTS

We are grateful to the Kentucky Lung Cancer Research Program (K.-B.K), for Kentucky Tobacco Research and Development Center grants, for a Research to Prevent Blindness Challenge grant (R.M.), and for the financial support of a University of Kentucky Graduate School Fellowship (Y.K.H.).

Received: August 9, 2006
Revised: February 9, 2007
Accepted: March 1, 2007
Published: April 27, 2007

REFERENCES

1. Deshaies, R.J. (1999). SCF and Cullin/Ring H2-based ubiquitin ligases. Annu. Rev. Cell Dev. Biol. *15*, 435–467.
2. Karin, M., and Ben-Neriah, Y. (2000). Phosphorylation meets ubiquitination: the control of NF-[κ]B activity. Annu. Rev. Immunol. *18*, 621–663.
3. Ciechanover, A., and Schwartz, A.L. (2002). Ubiquitin-mediated degradation of cellular proteins in health and disease. Hepatology *35*, 3–6.
4. Myung, J., Kim, K.B., Lindsten, K., Dantuma, N.P., and Crews, C.M. (2001). Lack of proteasome active site allostery as revealed by subunit-specific inhibitors. Mol. Cell *7*, 411–420.
5. Nazif, T., and Bogyo, M. (2001). Global analysis of proteasomal substrate specificity using positional-scanning libraries of covalent inhibitors. Proc. Natl. Acad. Sci. USA *98*, 2967–2972.
6. Loidl, G., Groll, M., Musiol, H.J., Ditzel, L., Huber, R., and Moroder, L. (1999). Bifunctional inhibitors of the trypsin-like activity of eukaryotic proteasomes. Chem. Biol. *6*, 197–204.
7. Loidl, G., Groll, M., Musiol, H.J., Huber, R., and Moroder, L. (1999). Bivalency as a principle for proteasome inhibition. Proc. Natl. Acad. Sci. USA *96*, 5418–5422.
8. Loidl, G., Musiol, H.J., Groll, M., Huber, R., and Moroder, L. (2000). Synthesis of bivalent inhibitors of eucaryotic proteasomes. J. Pept. Sci. *6*, 36–46.
9. Myung, J., Kim, K.B., and Crews, C.M. (2001). The ubiquitin-proteasome pathway and proteasome inhibitors. Med. Res. Rev. *21*, 245–273.
10. Kisselev, A.F., Callard, A., and Goldberg, A.L. (2006). Importance of the different proteolytic sites of the proteasome and the efficacy of inhibitors varies with the protein substrate. J. Biol. Chem. *281*, 8582–8590.
11. Crawford, L.J., Walker, B., Ovaa, H., Chauhan, D., Anderson, K.C., Morris, T.C., and Irvine, A.E. (2006). Comparative selectivity and specificity of the proteasome inhibitors BzLLLCOCHO, PS-341, and MG-132. Cancer Res. *66*, 6379–6386.
12. Montagut, C., Rovira, A., and Albanell, J. (2006). The proteasome: a novel target for anticancer therapy. Clin. Transl. Oncol. *8*, 313–317.
13. Chim, C.S., Ooi, G.C., Loong, F., Au, A.W., and Lie, A.K. (2005). Side effects and good effects from new chemotherapeutic agents. Case 3. Bortezomib in primary refractory plasmacytoma. J. Clin. Oncol. *23*, 2426–2428.
14. Kloetzel, P.M. (2001). Antigen processing by the proteasome. Nat. Rev. Mol. Cell Biol. *2*, 179–187.
15. Rock, K.L., and Goldberg, A.L. (1999). Degradation of cell proteins and the generation of MHC class I-presented peptides. Annu. Rev. Immunol. *17*, 739–779.
16. Fruh, K., Gossen, M., Wang, K., Bujard, H., Peterson, P.A., and Yang, Y. (1994). Displacement of housekeeping proteasome subunits by MHC-encoded LMPs: a newly discovered mechanism for modulating the multicatalytic proteinase complex. EMBO J. *13*, 3236–3244.
17. Strehl, B., Seifert, U., Kruger, E., Heink, S., Kuckelkorn, U., and Kloetzel, P.M. (2005). Interferon-γ, the functional plasticity of the ubiquitin-proteasome system, and MHC class I antigen processing. Immunol. Rev. *207*, 19–30.
18. Orlowski, R.Z. (2005). The ubiquitin proteasome pathway from bench to bedside. Hematology (Am. Soc. Hematol. Educ. Program) 220–225.
19. Voorhees, P.M., and Orlowski, R.Z. (2006). The proteasome and proteasome inhibitors in cancer therapy. Annu. Rev. Pharmacol. Toxicol. *46*, 189–213.
20. Casp, C.B., She, J.X., and McCormack, W.T. (2003). Genes of the LMP/TAP cluster are associated with the human autoimmune disease vitiligo. Genes Immun. *4*, 492–499.
21. Diaz-Hernandez, M., Hernandez, F., Martin-Aparicio, E., Gomez-Ramos, P., Moran, M.A., Castano, J.G., Ferrer, I., Avila, J., and Lucas, J.J. (2003). Neuronal induction of the immunoproteasome in Huntington's disease. J. Neurosci. *23*, 11653–11661.
22. Piccinini, M., Mostert, M., Croce, S., Baldovino, S., Papotti, M., and Rinaudo, M.T. (2003). Interferon-γ-inducible subunits are incorporated in human brain 20S proteasome. J. Neuroimmunol. *135*, 135–140.
23. Noda, C., Tanahashi, N., Shimbara, N., Hendil, K.B., and Tanaka, K. (2000). Tissue distribution of constitutive proteasomes, immunoproteasomes, and PA28 in rats. Biochem. Biophys. Res. Commun. *277*, 348–354.
24. Mishto, M., Bellavista, E., Santoro, A., Stolzing, A., Ligorio, C., Nacmias, B., Spazzafumo, L., Chiappelli, M., Licastro, F., Sorbi, S., et al. (2006). Immunoproteasome and LMP2 polymorphism in aged and Alzheimer's disease brains. Neurobiol. Aging *27*, 54–66.
25. Zhang, H., Sun, L., Liang, J., Yu, W., Zhang, Y., Wang, Y., Chen, Y., Li, R., Sun, X., and Shang, Y. (2006). The catalytic subunit of the proteasome is engaged in the entire process of estrogen receptor-regulated transcription. EMBO J. *25*, 4223–4233.
26. Singhal, S., and Mehta, J. (2003). Novel therapies in multiple myeloma. Int. J. Hematol. *77*, 226–231.
27. Hideshima, T., Chauhan, D., Podar, K., Schlossman, R.L., Richardson, P., and Anderson, K.C. (2001). Novel therapies targeting the myeloma cell and its bone marrow microenvironment. Semin. Oncol. *28*, 607–612.
28. Hideshima, T., Chauhan, D., Hayashi, T., Akiyama, M., Mitsiades, N., Mitsiades, C., Podar, K., Munshi, N.C., Richardson, P.G., and Anderson, K.C. (2003). Proteasome inhibitor PS-341 abrogates IL-6 triggered signaling cascades via caspase-dependent downregulation of gp130 in multiple myeloma. Oncogene *22*, 8386–8393.
29. Hideshima, T., and Anderson, K.C. (2002). Molecular mechanisms of novel therapeutic approaches for multiple myeloma. Nat. Rev. Cancer *2*, 927–937.
30. Altun, M., Galardy, P.J., Shringarpure, R., Hideshima, T., LeBlanc, R., Anderson, K.C., Ploegh, H.L., and Kessler, B.M. (2005). Effects

of PS-341 on the activity and composition of proteasomes in multiple myeloma cells. Cancer Res. *65*, 7896–7901.

31. Meng, L., Kwok, B.H., Sin, N., and Crews, C.M. (1999). Eponemycin exerts its antitumor effect through the inhibition of proteasome function. Cancer Res. *59*, 2798–2801.
32. Meng, L., Mohan, R., Kwok, B.H., Elofsson, M., Sin, N., and Crews, C.M. (1999). Epoxomicin, a potent and selective proteasome inhibitor, exhibits in vivo antiinflammatory activity. Proc. Natl. Acad. Sci. USA *96*, 10403–10408.
33. Kim, K.B., Myung, J., Sin, N., and Crews, C.M. (1999). Proteasome inhibition by the natural products epoxomicin and dihydroeponemycin: insights into specificity and potency. Bioorg. Med. Chem. Lett. *9*, 3335–3340.
34. Kuttler, C., Nussbaum, A.K., Dick, T.P., Rammensee, H.G., Schild, H., and Hadeler, K.P. (2000). An algorithm for the prediction of proteasomal cleavages. J. Mol. Biol. *298*, 417–429.
35. Ho, A., Cyrus, K., and Kim, K.B. (2005). Towards immunoproteasome-specific inhibitors: an improved synthesis of dihydroeponemycin. Eur. J. Org. Chem. *2005*, 4829–4834.
36. Groll, M., Kim, K.B., Kairies, N., Huber, R., and Crews, C.M. (2000). Crystal structure of epoxomicin: 20S proteasome reveals a molecular basis for selectivity of a′,b′-epoxyketone proteasome inhibitors. J. Am. Chem. Soc. *122*, 1237–1238.
37. Lowe, J., Stock, D., Jap, B., Zwickl, P., Baumeister, W., and Huber, R. (1995). Crystal structure of the 20S proteasome from the archaeon *T. acidophilum* at 3.4 Å resolution. Science *268*, 533–539.
38. Groll, M., Ditzel, L., Lowe, J., Stock, D., Bochtler, M., Bartunik, H.D., and Huber, R. (1997). Structure of 20S proteasome from yeast at 2.4 Å resolution. Nature *386*, 463–471.
39. Eleuteri, A.M., Kohanski, R.A., Cardozo, C., and Orlowski, M. (1997). Bovine spleen multicatalytic proteinase complex (proteasome). Replacement of X, Y, and Z subunits by LMP7, LMP2, and MECL1 and changes in properties and specificity. J. Biol. Chem. *272*, 11824–11831.
40. Cardozo, C., and Kohanski, R.A. (1998). Altered properties of the branched chain amino acid-preferring activity contribute to increased cleavages after branched chain residues by the "immunoproteasome". J. Biol. Chem. *273*, 16764–16770.
41. Craiu, A., Gaczynska, M., Akopian, T., Gramm, C.F., Fenteany, G., Goldberg, A.L., and Rock, K.L. (1997). Lactacystin and clasto-lactacystin β-lactone modify multiple proteasome β-subunits and inhibit intracellular protein degradation and major histocompatibility complex class I antigen presentation. J. Biol. Chem. *272*, 13437–13445.
42. Reidlinger, J., Pike, A.M., Savory, P.J., Murray, R.Z., and Rivett, A.J. (1997). Catalytic properties of 26 S and 20 S proteasomes and radiolabeling of MB1, LMP7, and C7 subunits associated with trypsin-like and chymotrypsin-like activities. J. Biol. Chem. *272*, 24899–24905.
43. Cardozo, C., Eleuteri, A.M., and Orlowski, M. (1995). Differences in catalytic activities and subunit pattern of multicatalytic proteinase complexes (proteasomes) isolated from bovine pituitary, lung, and liver. Changes in LMP7 and the component necessary for expression of the chymotrypsin-like activity. J. Biol. Chem. *270*, 22645–22651.
44. Salzmann, U., Kral, S., Braun, B., Standera, S., Schmidt, M., Kloetzel, P.M., and Sijts, A. (1999). Mutational analysis of subunit i β2 (MECL-1) demonstrates conservation of cleavage specificity between yeast and mammalian proteasomes. FEBS Lett. *454*, 11–15.
45. Basler, M., Moebius, J., Elenich, L., Groettrup, M., and Monaco, J.J. (2006). An altered T cell repertoire in MECL-1-deficient mice. J. Immunol. *176*, 6665–6672.
46. Mohan, R., Hammers, H.J., Bargagna-Mohan, P., Zhan, X.H., Herbstritt, C.J., Ruiz, A., Zhang, L., Hanson, A.D., Conner, B.P., Rougas, J., and Pribluda, V.S. (2004). Withaferin A is a potent inhibitor of angiogenesis. Angiogenesis *7*, 115–122.
47. Korff, T., and Augustin, H.G. (1998). Integration of endothelial cells in multicellular spheroids prevents apoptosis and induces differentiation. J. Cell Biol. *143*, 1341–1352.
48. Bargagna-Mohan, P., Ravindranath, P.P., and Mohan, R. (2006). Small molecule anti-angiogenic probes of the ubiquitin proteasome pathway: potential application to choroidal neovascularization. Invest. Ophthalmol. Vis. Sci. *47*, 4138–4145.
49. Griffin, T.A., Nandi, D., Cruz, M., Fehling, H.J., Kaer, L.V., Monaco, J.J., and Colbert, R.A. (1998). Immunoproteasome assembly: cooperative incorporation of interferon γ (IFN-γ)-inducible subunits. J. Exp. Med. *187*, 97–104.
50. Kingsbury, D.J., Griffin, T.A., and Colbert, R.A. (2000). Novel propeptide function in 20 S proteasome assembly influences beta subunit composition. J. Biol. Chem. *275*, 24156–24162.
51. De, M., Jayarapu, K., Elenich, L., Monaco, J.J., Colbert, R.A., and Griffin, T.A. (2003). Beta 2 subunit propeptides influence cooperative proteasome assembly. J. Biol. Chem. *278*, 6153–6159.

